Acta Universitatis Sapientiae
Electrical and Mechanical Engineering, 3 (2011) 93-104

Study of the Edge Profile Variation Caused by the Re-sharpening by Profiled Milling Heads with Cutting Inserts

Márton MÁTÉ, Dénes HOLLANDA

Department of Mechanical Engineering, Faculty of Technical and Human Sciences,
Sapientia Hungarian University of Transylvania, Tg. Mureş
e-mail: mmate@ms.sapientia.ro, hollanda@ms.sapientia.ro

Manuscript received October 04, 2011; revised December 18, 2011.

Abstract: The paper presents the calculus of the cut profile and the variation of this caused by the re-sharpening, that appears by a special profiled milling head construction, that uses cutting inserts. The advantage of the proposed milling head versus the classical concave profiled milling disk is evident, if considering the repartition of the cutting speed vector and the chip forming and exhausting conditions. The cutting insert's rake face is plain. Its relief face is a part of a common thorus realized by grinding. The insert occupies two distinct positions in the body of the tool: one for cutting and the other one for re-sharpening. Indexed positions are ensured through conical holes and corresponding slotted head sets. The re-sharpening can be done on the rake face or on the relief face. In both cases a minor profile error occurs but the profile is kept in the limits of the tolerance. This paper discusses the definition of the profile error and its dependence on the angular setting parameters and the number of the re-sharpening. The final conclusion is that the classical concave profiled milling disk can be replaced with the proposed variant.

Keywords: Profile milling, profiled milling head profile error, inserts, geometry.

1. The assembly of the profiled milling head

Profiled milling, especially in cases of convex profiles, is a difficult operation. The classical concave profiled disk mills present low rigidity on the teeth base [2, 3, 4, 5] and as a consequence, the cutting speed and feed cannot be set to high values. The productivity of operation is low and the surface roughness, due to the small rake angle values in most of the cases results just on the limit. Profiled disc mills are rather expensive due to the relieving operation.

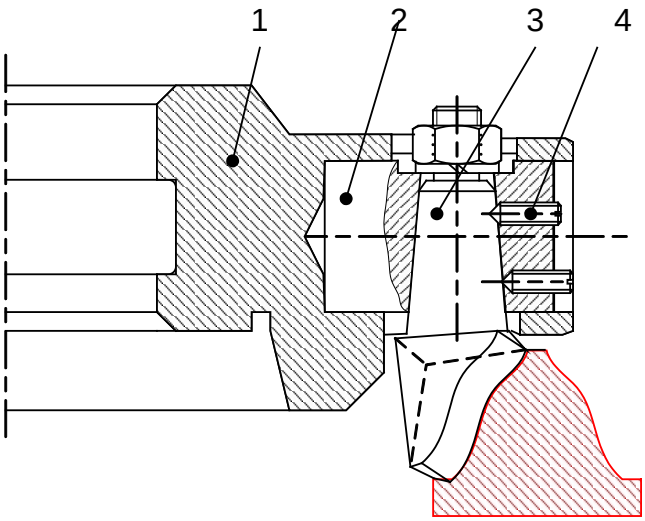

Figure 1: The profiled milling head.

An alternative to the profiled milling disks can be realized with a milling head that includes profiled cutting inserts (*Fig.1)*. The body (1) of the milling head contains 6-8 radially disposed holders (2), where the holder's axes intersect the rotation axis of the body. The holder contains the profiled cutting insert (3).

Holders and inserts can be set at certain angular positions due to the positioning slotted head sets (4). The insert and the holder can be set in two certain positions: the first for profiling and /or re-sharpening, and the second for cutting. When cutting, the holder is turned away with the angle α_T for ensuring the top relief angle, and the insert in the holder is also rotated with α_s in order to realize the side relief angle as shown in *Fig. 2*. The relief faces of the inserts are subsets of a common revolved surface, where the axis of revolution coincides with the axis of the milling head.

Paper [1] presents two calculus procedures for determining the profile of the grinding disk that realizes the relief faces of the inserts. Starting from the parametric equations of the workpiece profile, first the cutting edge in work position is calculated. Rotating the insert and its holder to the profiling /re-sharpening position, the profile of the grinding tool is calculated.

The re-sharpening of the insert can be done in two ways:

a. on the rake face, analogously to the re-sharpening of profiled turning disks, separately for each insert;
b. on the relief face, by profile grinding, simultaneously for all inserts.

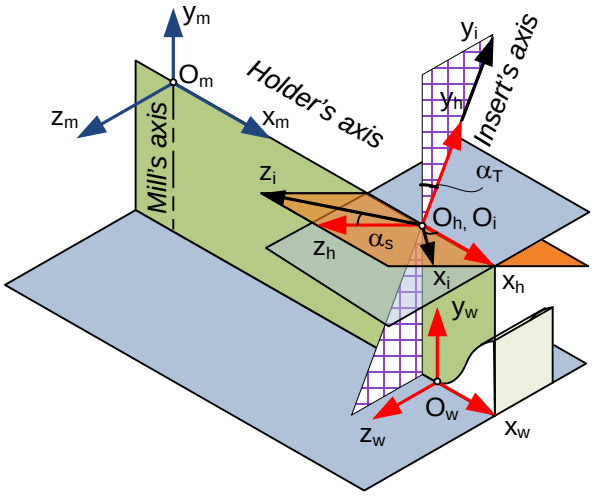

Figure 2: The geometrical model of the milling head – the attached coordinate-systems.

However, the new cutting edge moves in a new position, correlated to the insert's axis. When the insert and the holder are turned back in the cutting position, the cutting edge generates a revolved surface with a different axial section, despite the fact, that its shape remains invariant. In conclusion, profile error occurs.

In the following, the evolution of the profile error in the case of re-sharpening on the rake face will be analyzed.

2. The mathematical model of the cutting edge

Let's consider the geometric model of the milling head, with the coordinate-systems attached to the rigid body and to the mobile components as shown in *Fig. 2*. System $\mathbf{S}_m\{O_m x_m y_m z_m\}$ attached to the body, is used to define the equations of the cutting edge, the grinding wheel profile and the cut profile. System $\mathbf{S}_h\{O_h x_h y_h z_h\}$ of the holder is turned about axis x_h with angle α_T, while the system $\mathbf{S}_i\{O_i x_i y_i z_i\}$ of the insert is rotated about axis y_h with angle α_s. When the insert and the holder occupy the re-sharpening position, all axes are parallel with the corresponding axes of $\mathbf{S}_m$. Starting from the parametric coordinates $(\varphi(u),\psi(u),0)$ of the workpiece profile given in the workpiece

system $\mathbf{S}_w\{O_w x_w y_w z_w\}$ and applying the necessary coordinate transformations as shown in [1], there result the equations of the cutting edge. Omitting the calculus, the edge's equations in the $\mathbf{S}_m$ system are

$$\begin{cases} x_m^{(e)}(u) = (\varphi(u) + R_0 + \Delta)\cos\theta(u) \\ y_m^{(e)}(u) = \psi(u) \\ z_m^{(e)}(u) = (\varphi(u) + R_0 + \Delta)\sin\theta(u) \end{cases} \tag{1}$$

where the function $\theta(u)$ is obtained from the equations of the revolved generating surface of the milling head and the rake face, positioned for cutting (α_T and α_s are set to their cutting values):

$$\theta(u) = \arcsin\frac{R_0\tan(\gamma_0 - \alpha_s) - (\psi(u) - H)\sin\alpha_T}{(\varphi(u) + R_0 + \Delta)\cos\alpha_T} - \arctan\left(\frac{\tan(\gamma_0 - \alpha_s)}{\cos\alpha_T}\right) \tag{2}$$

With this, the new cutting edge is completely determined.

Now it is necessary to model how the cutting edge position and/or shape will change after the re-sharpening process.

3. The profile variation by re-sharpening on the rake face

The re-sharpening on the rake face consists in the renewal of the rake plane, conserving the shape of the cutting edge. This procedure is executed when the insert and the holder are turned in the re-sharpening position characterized by the zero value of α_T and α_s. The rake face in the re-sharpening position is parallel with the mill's axis of rotation. After the re-sharpening it will occupy a new position that is rotated away from the first position with angle λ as shown in *Fig. 3.*

First the equations of the edge have to be rewritten in the insert's system. Denoting with $\mathbf{r}_i^{(e)}$ the homogeneous coordinates of the cutting edge in the insert's system, and $\mathbf{r}_m^{(e)}$ the same coordinates in the mill's system, it can be written that

$$\mathbf{r}_i^{(e)} = \mathbf{M}_{im}\mathbf{r}_m^{(e)} = \begin{pmatrix} \cos\alpha_s & \sin\alpha_T\sin\alpha_s & \cos\alpha_T\sin\alpha_s & -R_0\cos\alpha_s \\ 0 & \cos\alpha_T & -\sin\alpha_T & 0 \\ -\sin\alpha_s & \sin\alpha_T\cos\alpha_s & \cos\alpha_T\cos\alpha_s & R_0\sin\alpha_s \\ 0 & 0 & 0 & 1 \end{pmatrix}\mathbf{r}_m^{(e)}. \tag{3}$$

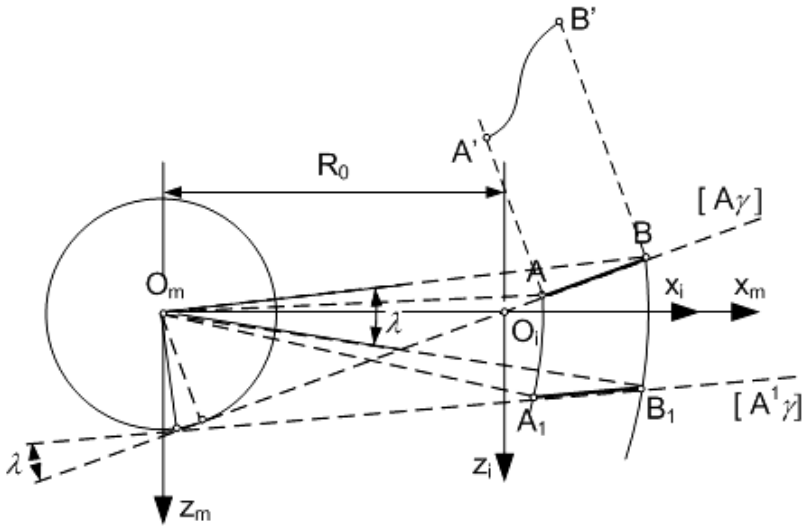

Figure 3: The rake face before and after re-sharpening.

Now let's turn the holder and the insert in re-sharpening position. Due to zero values of α_T and α_s in this position, the $\mathbf{M}_{im}$ matrix reduces to a translation matrix. Using $\mathbf{M}_{mi}$, the inverted matrix of $\mathbf{M}_{im}$, the equations of the rotated edge in $\mathbf{S}_m$ result as follows:

$$\begin{cases} x_m^{(e*)}(u) = x_i^{(e)}(u) + R_0 \\ y_m^{(e*)}(u) = y_i^{(e)}(u) \\ z_m^{(e*)}(u) = z_i^{(e)}(u) \end{cases} . \tag{4}$$

According to *Fig. 3*, this corresponds to zero value of the rake face position angle λ. The generalized cutting edge equations, depend on the state of re-sharpening given by λ:

$$\begin{cases} x_m^{(e1)}(u,\lambda) = -x_m^{(e*)}(u)\sin\lambda + z_m^{(e*)}(u)\cos\lambda \\ y_m^{(e1)}(u,\lambda) = y_m^{(e*)}(u) \\ z_m^{(e1)}(u,\lambda) = x_m^{(e*)}(u)\cos\lambda + z_m^{(e*)}(u)\sin\lambda \end{cases} . \tag{5}$$

This new edge must be turned now in the working position. For that, it is necessary to write its equations in the system of the insert, applying a translation along axis x_m. Using the coordinate functions (5), it results:

$$\mathbf{r}_i^{(e1)} = \begin{pmatrix} x_i^{(e1)} \\ y_i^{(e1)} \\ z_i^{(e1)} \\ 1 \end{pmatrix} = \begin{pmatrix} x_m^{(e1)} - R_0 \\ y_m^{(e1)} \\ z_m^{(e1)} \\ 1 \end{pmatrix}. \tag{6}$$

Now the cutting edge is turned back in working position. Let's denote with $\mathbf{r}_m^{(ge)}$ the vector of homogeneous coordinates of the re-sharpened cutting edge. Using again the transformation matrix from (3), it results:

$$\mathbf{r}_m^{(eg)} = \begin{pmatrix} x_m^{(ge)} \\ y_m^{(ge)} \\ z_m^{(ge)} \\ 1 \end{pmatrix} = \mathbf{M}_{mi}\mathbf{r}_i^{(e1)}. \tag{7}$$

Finally, the equations of the generated profile in the $\boldsymbol{S}_m$ system are given by the expressions:

$$\begin{cases} x_m^{(pr)} = \sqrt{\left[x_m^{(ge)}\right]^2 + \left[x_m^{(ge)}\right]^2} \\ y_m^{(pr)} = y_m^{(ge)} \\ z_m^{(pr)} = 0 \end{cases}. \tag{8}$$

4. The modeling of the profile error

The profile error can be calculated in many different ways. However, all models must correspond to the definition of the profile error [7] given by the corresponding standards [6]. The calculus is based on the hypotheses that profile error occurs, because the edge points change their position after re-sharpening. First calculus method tries to compute the average of the displacements. The comparison is made between the new generating profile and the translated theoretical workpiece profile. The translated theoretical workpiece profile coincides with the original one, but translation is realized in order to get the best approximant for the new generating profile.

As well shown in Fig. 4a, the original workpiece profile AB (generated by the new edge) is translated by parameters (a,b) to the position A^*B^*. The profile generated by the new edge is A_1B_1. Considering a set of N discrete points on the original profile defined by the certain values of parameter u, it

has to remarked that a given point M_i moves to M_i^*. With this, the local profile error is considered the distance $\overline{M_iM_i^*}$. The nominal value of the profile error is the maximum value encountered by the distance $\overline{M_iM_i^*}$ along the edge. The translation parameters (a,b) are calculated using the least squares method.

Fig.4b shows the definition of the profile error in the normal direction. The equations of the translated workpiece profile are:

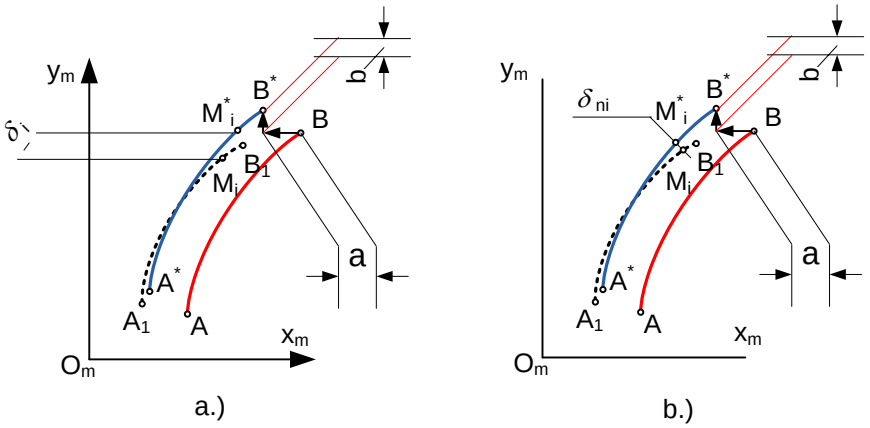

Figure 4: The modeling of the profile errors.

$$\begin{cases} x(u) = (\varphi(u) + R_0 + \Delta) + a \\ y(u) = \psi(u) + b \end{cases}. \tag{9}$$

The equation of the normal line started from the profile point $M_i^*(x_i^*, y_i^*)$ to the workpiece profile given by equations (9) is

$$(x_i^* - x(u))\dot{\varphi}(u) + (y_i^* - y(u))\psi(u) = 0 \tag{10}$$

and admits the root u_i. With this, the local normal error is defined through the distance $\overline{M_iM_i^*}$ on *Fig 4b*:

$$\delta_i^n = \sqrt{(x_i^* - x(u_i))^2 + (y_i^* - y(u_i))^2} \quad . \tag{11}$$

5. Numerical approach

In order to emphasize the evolution of the profile errors occurring by re-sharpening, let's consider a practical example. The workpiece profile is a parabola (*Fig. 5*) described by the equations

$$\begin{cases} x(u) \equiv \varphi(u) = u \\ y(u) = \psi(u) = -\dfrac{3}{20}u^2 + \dfrac{47}{20}u, \qquad u \in [0,5] \end{cases} \tag{12}$$

The reference radius of the insert is set to $R_0 = 100\,\text{mm}$, and the approximate value of distance of the edge-top to the axis of the insert, along axis x is $\Delta = 5\,\text{mm}$.

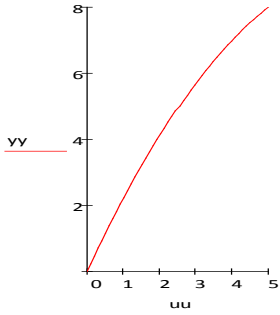

Figure 5: The workpiece profile.

The grinding allowance for the admissible wear of the relief face is considered $K_\alpha = 0{,}3mm$. After the re-sharpening, the new rake face rotates about axis z_m with $\Delta\lambda \approx K_\alpha / R_0 \approx 10'18{,}8''$ reported to its position before the grinding operation. Considering that the total grinding reserve of the insert is $A_\Sigma \approx 10\,mm$, it can be stated that the corresponding total rotation angle is $\lambda_\Sigma = A_\Sigma / R_0 \approx 5°43'46{,}5''$. According to this, the predicted number of re-sharpening becomes $N_{re} = [\lambda_\Sigma / \Delta\lambda] \approx 33$.

For studying the evolution of the profile errors according to the values of the angles γ_s, α_T and α_s, the proposed limits for their values are as follows:

$$\begin{aligned} 1° \le \alpha_T &\le 6° \\ 5° \le \alpha_s &\le 8° \\ 5° \le \gamma_s &\le 10° \end{aligned} \quad .$$

Angle γ_s is the conventional rake angle, that can be approximated by $\gamma_s \approx \gamma_0 - \alpha_s$. When the influence of one parameter is studied, the others are set to the middle of their interval: $\overline{\alpha}_T = 3°30'; \overline{\alpha}_s = 6°30'; \overline{\gamma}_s = 7°30'$. The simulation program calculates for each parameter combination and each state of re-sharpening, the evolution of the errors along the profile. Both types of errors mentioned in section 4 are calculated. The conclusion is that the shapes of error evolution diagrams are not significantly different. As follows, a consistent conclusion can be deduced studying only the normal errors.

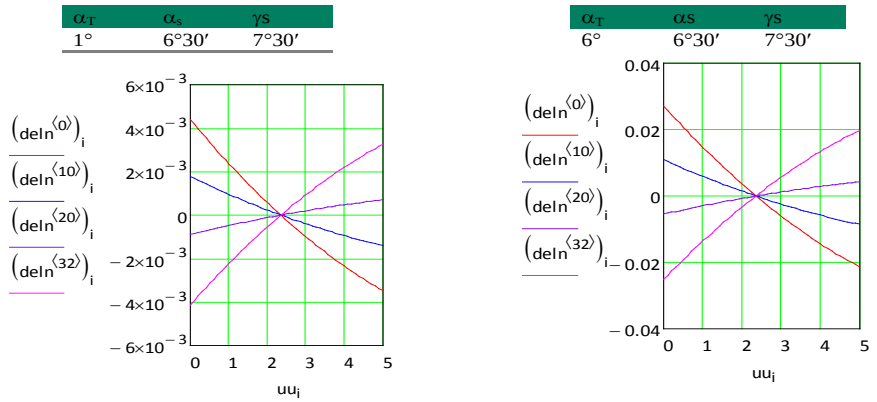

Figure 6: The evolution of the normal errors along the edge for different settings of α_T parameter and different states of re-sharpening.

Fig. 6 shows the evolution of the normal profile errors for the lowest and the highest value of the top relief angle α_T while α_s and γ_s are set to the median values. The horizontal axis contains the abscissa of discrete profile points ($N = 50$ points have been considered). The vertical axis contains the normal errors in millimeters, for different numbers of re-sharpening. The index $\langle 0 \rangle$ denotes the first, and the index $\langle 32 \rangle$ the last re-sharpening. It can be observed that the evolution of errors is the same for both cases. First, error is decreasing till the number of the re-sharpenings increases to approximately the half of its maximum. This error variation is obtained due to the fact, that the new cutting edge is turned away from its theoretical position with $-\lambda_\Sigma / 2$. The same technique of manufacturing is used to maintain the errors in the limits of tolerance by the gear cutting hobs [2, 3, 4, 5]. Due to the optimal positioning of the etalon curve, the errors encounter the maximum values at the endpoints of the edge. It is to remark that α_T has a severe influence on the profile error. The

right-side diagram shows approximately four times larger maximum error values when α_T increases to 6° representing the upper limit considered for this angle.

When studying the influence of the other two angular parameters α_s and γ_s it can be observed that variation of the maximum error values is theoretically zero. The error diagrams are presented in *Fig. 7*. The same evolution is encountered when the influence of γ_s is studied.

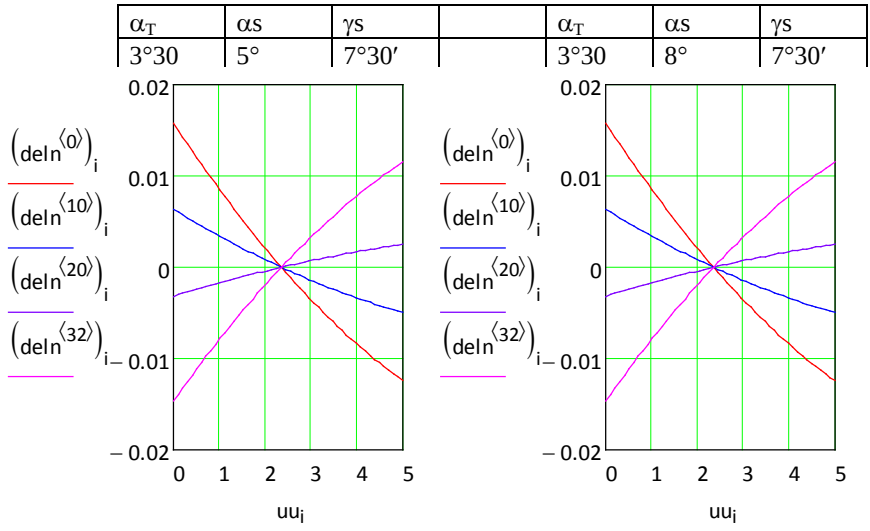

Figure 7: The influence of α_s parameter on the evolution of maximum value of profile error.

To ascertain the precision of the milling head it is necessary to calculate the maximum value of the errors. The computing routine is that used for outputting the drawings presented before. The results corresponding to the set values of the angular parameters α_T, α_s and γ_s are given in the table below.

Table 1: The evolution of the maximum error values.

α_T [°]	α_s [°]	γ_s [°]	γ_0 [°]	δ_{max} [mm]	δ^n_{max} [mm]
1	6,5	7,5	14	0,007934	0,007377
2	6,5	7,5	14	0,01613	0,01486
3	6,5	7,5	14	0,02433	0,02236
4	6,5	7,5	14	0,03254	0,02985
5	6,5	7,5	14	0,04075	0,03735
6	6,5	7,5	14	0,04897	0,04485
3,5	5	7,5	12,5	0,02857	0,02617
3,5	6	7,5	13,5	0,02848	0,02613
3,5	7	7,5	14,5	0,02838	0,02608
3,5	8	7,5	15,5	0,02826	0,02601
3,5	6,5	5	11,5	0,02851	0,02612
3,5	6,5	6	12,5	0,02848	0,02612
3,5	6,5	7	13,5	0,02845	0,02611
3,5	6,5	8	14,5	0,02842	0,0261

Considering just the shadowed part of the above table and represen-ting the last two columns versus the first it can be remarked that the variation of error is very close to linear (*Fig. 8*).

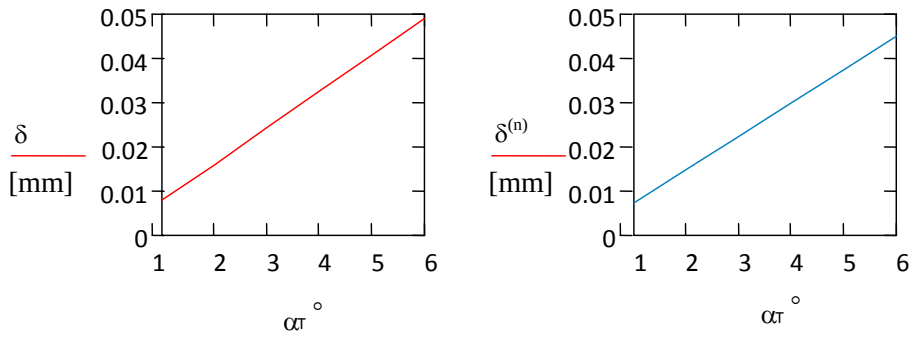

Figure 8: The linear dependence of the maximum profile error values on the top relief angle.

Performing a statistical analysis in order to establish the linear regression between the value of α_T and the corresponding value of the error, the following results were obtained:

$$\delta(\alpha_T) = -2.82666666667 \cdot 10^{-4}\,\alpha_T + 8.20714285714 \cdot 10^{-3} \qquad (13)$$

with a correlation coefficient of $c = 0.999999868303$ and a standard error $\sigma = 8.81 \cdot 10^{-6}$. Considering the normal error, the results are very slightly different:

$$\delta^{(n)}(\alpha_T) = -1.24666666667 \cdot 10^{-4} \alpha_T + 7.49500000000 \cdot 10^{-3} \qquad (14)$$

with a correlation coefficient of $c = 0.999999937271$ and a standard error $\sigma = 5.553 \cdot 10^{-6}$.

Conclusions

Analyzing the diagrams and the results presented before, the following conclusions can be established:

- the unique probable influence on the variation of the milling head profile precision due to the re-sharpening, is caused by the top relief angle α_T;
- the value of the top relief angle can be set smaller than 2°, that will lead to maximum profile errors less than 10μm;
- a profiled cutting tool construction with sufficient precision can be realized without applying the classical and pretty complicated relieving operation;
- relief faces are easily realizable through NC grinding, simultaneously for all inserts.

References

[1] Máté, M., and Hollanda, D., "A Possible Concept of Peripheral Edged Profile Mills for External Convex Profiles", in *Proc. of the IMC 2011-International Multidisciplinary Conference, 9-th Edition, Nyíregyháza*, May 19-21, 2011, pp. 173-178.

[2] Hollanda, D. , "Aşchiere şi scule", Universitatea din Braşov, 1983.

[3] Secară, Gh., "Proiectarea sculelor aşchietoare", Ed. Didactică şi Pedag. Bucureşti, 1979.

[4] Hollanda, D., Máté, M., "Aşchiere şi scule", Ed. Univ. „Petru Maior", Tîrgu-Mureş, 2003.

[5] Belous, V., "Sinteza sculelor aşchietoare", Editura Junimea, Iaşi, 1980.

[6] Y14.5.1M-1994 (R2004), "Mathematical Definition Of Dimensioning And Tolerancing Principles", ASME International Standards.

[7] Pasupathy, T. M. K., Wilhelm, R. G., Gregory, A. H., "Profile tolerance zones with control points", http://www.aspe.net/publications/, Annual_2000/PDF/ POSTERS/ METROL / FORM/.

[8] Maestre, J. M., Munoz de la Pena, D. and Camacho, E. F., "Distributed MPC: a supply chain case study", *IEEE Conference on Decision and Control, Shanghai, China*, December 16-18, 2009, pp. 7099 – 7104.

[9] Venkat, A. N., Hiskens, I. A., Rawlings, J. B. and Wright, S. J. "Distributed MPC Strategies With Application to Power System Automatic Generation Control", *IEEE Transactions on Control Systems Technology*, vol. 16, no. 6, pp. 1192-1206, November, 2008.